



Article

Synthesis, characterisation and bioconjugation of [109Cd]CdSe/ZnS core/shell quantum dots as “proof of principle” for the potential development of an anti-cancer theranostic

Gillies, James Millar

Available at <http://clock.uclan.ac.uk/29160/>

Gillies, James Millar ORCID: 0000-0002-9956-509X (2019) Synthesis, characterisation and bioconjugation of [109Cd]CdSe/ZnS core/shell quantum dots as “proof of principle” for the potential development of an anti-cancer theranostic. Inorganica Chimica Acta, 495 . p. 119001. ISSN 0020-1693

It is advisable to refer to the publisher’s version if you intend to cite from the work.
<http://dx.doi.org/10.1016/j.ica.2019.119001>

For more information about UCLan’s research in this area go to <http://www.uclan.ac.uk/researchgroups/> and search for <name of research Group>.

For information about Research generally at UCLan please go to <http://www.uclan.ac.uk/research/>

All outputs in CLoK are protected by Intellectual Property Rights law, including Copyright law. Copyright, IPR and Moral Rights for the works on this site are retained by the individual authors and/or other copyright owners. Terms and conditions for use of this material are defined in the [policies](#) page.

Accepted Manuscript

Synthesis, characterisation and bioconjugation of [^{109}Cd]CdSe/ZnS core/shell quantum dots as “proof of principle” for the potential development of an anti-cancer theranostic

J.M. Gillies

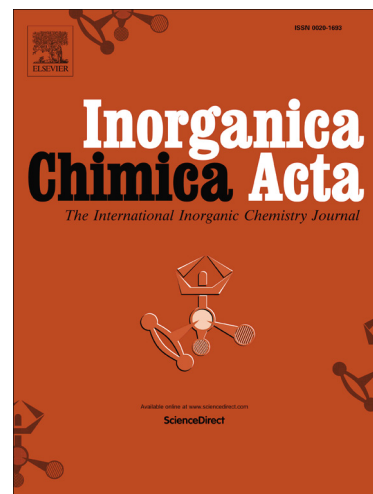
PII: S0020-1693(19)30593-6
DOI: <https://doi.org/10.1016/j.ica.2019.119001>
Article Number: 119001
Reference: ICA 119001

To appear in: *Inorganica Chimica Acta*

Received Date: 25 March 2019
Revised Date: 3 July 2019
Accepted Date: 4 July 2019

Please cite this article as: J.M. Gillies, Synthesis, characterisation and bioconjugation of [^{109}Cd]CdSe/ZnS core/shell quantum dots as “proof of principle” for the potential development of an anti-cancer theranostic, *Inorganica Chimica Acta* (2019), doi: <https://doi.org/10.1016/j.ica.2019.119001>

This is a PDF file of an unedited manuscript that has been accepted for publication. As a service to our customers we are providing this early version of the manuscript. The manuscript will undergo copyediting, typesetting, and review of the resulting proof before it is published in its final form. Please note that during the production process errors may be discovered which could affect the content, and all legal disclaimers that apply to the journal pertain.



Synthesis, characterisation and bioconjugation of [¹⁰⁹Cd]CdSe/ZnS core/shell quantum dots as “proof of principle” for the potential development of an anti-cancer theranostic.

J . M. Gillies

Cancer Research-UK/University of Manchester, Manchester, M13 9PL

Address for corrispondance: jmgillies@uclan.ac.uk

School of Pharmacy and Biomedical Sciences,

University of Central Lancashire,

Preston,

Lancashire,

PR1 2HE.

Keywords: Radiochemistry, Nanocrystals, Multimodality Imaging, Rituximab, Theranostics.

Abstract

This work describes the synthesis and analysis of radioactive multifunctional nanoparticle probes based on CdSe/ZnS semiconductor quantum dots (QDs) for potential *in vitro* and *in vivo* anti-cancer theranostics. The synthetic design involved the radiosynthesis of luminescent CdSe/ZnS QDs using the SPECT imaging agent Cd-109 as the cadmium elemental source. These radioactive nanoparticle materials were then rendered water dispersed and bioconjugated to the tumor-targeting ligand Rituximab.

Introduction

The term “Theranostics” is commonly used to define the development of specific individualised therapies for a range of medical conditions, such as tumour diagnosis and therapy. Theranostics serves to combine diagnosis and therapy into a single tool[1]. The concept of cancer theranostics arose from the observation that cancer tumours are naturally heterogeneous in nature, that is, no two tumours, even in the same patient, will respond the same way to the same general treatment[2]. Therefore, a system needed to be developed where diagnosis and treatment could be performed on an individual tumour basis.

The goal of targeted theranostics is to create platforms that are specifically designed to provide more effective tumour imaging while reducing the degree of toxicity administered to healthy tissue during tumour treatment[2,3]. Nanoparticle research offers the possibility of a platform incorporating a combined real-time imaging and targeted therapy in one, with multiple novel capabilities. Nanoparticles have been shown to have the potential to be a more effective and selective delivery platform for therapeutics into tumour sites than conventional drug delivery systems[4-11].

Nanoparticles are nanometer scale particles made of either inorganic metal compounds[12] or polymer materials[13]. They are molecules composed of atoms from group II-VI (CdSe, CdTe, CdS) or III-V (InP, InAs) elements in the periodic table[13,14]. Their composition and small size (a few hundred to a few thousand atoms) give these particles powerful fluorescent and optical properties that can be readily customized by changing the size or composition of the nanoparticle[12]. Nanoparticles absorb light of a lower wavelength, then quickly re-emit the light but in a higher specific narrow wavelength[4-11].

Nanoparticles have many unique optical properties. The most striking property is that the colour of the absorption and emission, created from the nanoparticle, can be tuned to any chosen wavelength by simply changing their size[13-15].

Previously, nanoparticles have been developed for cancer tumour imaging, based on their ability to act as tagged fluorescent markers[10-12]. These nanoparticles can be selectively functionalised in order to bind to a range of biomolecules (proteins, peptides, nucleic acids, antibodies, etc.)[16,17]. Once functionalised the nanoparticles can be localised in tumour cells through a number of mechanisms including for example, receptor binding, enzyme activation, and expression of a specific gene product[18-20]. The nanoparticles give distinct intense localised fluorescence, depending on the wavelength of the light emitted, allowing the optical imaging of several pathways associated with the tumour and its environment.

The development of nanoparticles have become promising tools as fluorescence markers in various diagnostic applications and they have also been suggested as drug delivery vehicles with the purpose of achieving a high therapeutic index[5]. However, in all the *in vivo* applications described so far, high concentrations (10-100mg/ml) of nanoparticles have been used and this has raised major issues over toxicity, particularly of cadmium based nanoparticles. The data generated here shows the development of tracer quantities of radioactive nanoparticles that are synthesised using radioisotopes, such as the single photon emission computer tomographic (SPECT) imaging agents, Cadmium-109 ($t_{1/2} = 462.6\text{d}$, 88KeV γ -ray) or Selenium-70 ($t_{1/2} = 41.1\text{m}$, β^+). Such tracer radioactive nanoparticles will overcome the potential toxicity of the administration of cadmium based nanoparticles whilst maintaining the therapeutic and imaging functionalities of these particles.

The development of nanoparticles at both carrier added (containing both stable and radioactive isotope) and tracer levels (radioisotope only) from radioisotopes of the same elements as those used in the synthesis of conventional nanoparticle quantum dots[13-15]. Synthesis at the tracer level will allow the exploration of these inorganic metals as combined imaging and therapeutic agents, both in their radioactive form, for instance γ -emitters localised in tumour cells, and in their chemotherapeutic form, for example, toxic decay products created by the nanoparticle breakdown or by the nanoparticle release of toxic daughter isotopes.

Experimental

Materials

All reagents were purchased from Sigma-Aldrich U.K. unless otherwise indicated. Cadmium-109 was purchased from Amersham Biosciences, U.K. UV analysis was carried out on a Cary 300 Bio UV-vis spectrophotometer (Agilent, U.S.A.), Fluorescence analysis was carried out using a Nanodrop ND-3300 fluorospectrometer (ThermoFisher, U.K.). SEM was carried out on a Topcon DS 130F field emission scanning electron microscope (Topcon Corporation, Tokyo, Japan). Gamma ray spectroscopy was carried out on a Gammavision-32 gamma ray spectrometer (ORTEK, U.K.).

Synthesis of Carrier added [^{109}Cd]CdSe

Highly fluorescent [^{109}Cd]CdSe nanoparticles were synthesised by procedures modified from those reported previously[13]. For a typical reaction, the mixture of 25.0mg, (0.2 mM) of cadmium oxide (CdO), 3.0 mL of 1-octadecene (ODE) containing 37 MBq, 1 mCi of cadmium-109 cadmium chloride ([^{109}Cd]CdCl

(10 μ M)), and 227.0mg, (0.8 mmol) of stearic acid in a 25 mL three-neck flask was heated to 200 °C for 10 min to obtain a colourless clear solution. Following cooling to room temperature, octadecylamine (ODA, 1.5 g) and 0.5 g of Tri-n-octylphosphine oxide (TOPO) were added into the flask. Under argon flow, this system was reheated to 280°C. At this temperature, a selenium solution made by dissolving 68mg, (2.0 mM) of Se in 2.0 mL of tri-butyl phosphine (TBP) and 1.5 mL of ODE was quickly injected. The crystalline growth temperature was then reduced to 250 °C. This reaction generated [¹⁰⁹Cd]CdSe nanoparticles of about 3.5-10.0 nm in size with the first absorption peak around 570 nm. The reaction mixture was allowed to cool to room temperature, and an extraction procedure involving the addition of methanol/heptane 1:1 was used to purify the nanoparticles from side products and unreacted precursors. The purified cadmium-109 cadmium selenide ([¹⁰⁹Cd]CdSe) solution in heptane was used as a stock solution.

Synthesis of tracer level [¹⁰⁹Cd]CdSe nanoparticles

The above procedure was repeated except that stable CdO was omitted from the reaction matrix and the only cadmium source was supplied by the 37 MBq, 1 mCi of [¹⁰⁹Cd]CdCl (10 μ M) added to the reaction melt.

Coating with Zinc sulphide (ZnS)

TOPO (5g) was added to a three necked flask under argon and heated to 200°C for 1 hour. The solution was then cooled to 60°C and 0.5 mL of Tri-n-octylphosphine (TOP) and the [¹⁰⁹Cd]CdSe in heptane added. This mixture was then heated under argon to 220 °C. A capping solution of 0.1 mM dimethylzinc and 0.1 mM hexamethyldisilathiane in 5 ml TOP was slowly added to the [¹⁰⁹Cd]CdSe

TOPO/TOP solution over a time course of 10 min at 220 °C. The reaction was heated at 220 °C for 30 min. The temperature was then reduced to 90°C for 2 hours. The [¹⁰⁹Cd]CdSe/ZnS nanoparticles formed had emission wavelength approximately 30 nm higher than the original [¹⁰⁹Cd]CdSe nanoparticles with excellent chemical and photo stability. The reaction mixture was then cooled to room temperature, and the dots were extracted with solvent methanol/heptane mixture (v/v 1:1).

Water dispersion of [¹⁰⁹Cd]CdSe

[¹⁰⁹Cd]CdSe[21] nanoparticles (100 µl TOPO coated in toluene) in a polypropylene vial were washed and centrifugally precipitated with 3 x 1ml of methanol at 9000g for 15 min. The final pellet was re-suspended in 50 µl of chloroform, to which 25 µl of mercaptoacetic acid, followed by 25 µl of tetramethylammonium hydroxide (25% solution in methanol) were added. After sealing the vial, the mixture was sonicated for 1 minute and allowed to stand overnight. The mixture was then maintained at 60°C in a water bath for one hour. At the end of this time the nanoparticles were centrifugally precipitated for ten minutes at 9000g. The supernatant was carefully removed, and then the pellet was washed with 2 x 1ml of methanol at 9000g for 15 minutes. The final pellet was suspended in 1 ml of 10 mM sodium bicarbonate solution and stored in the dark.

Direct reaction of [¹²⁵I]NaI with Rituximab

Iodine-125 (Amersham Pharmacia Biotech) was used for the development of the radiolabelling method for Rituximab and for animal biodistribution studies. Iodogen (1,3,4,6-tetrachloro-3 α ,6 α -diphenylglycouril, Sigma) was dissolved in dichloromethane (0.4 mg/ml) and dispensed into microfuge tubes (20 µl in 0.5 ml

tubes; 80 μ l in 1.5 ml tubes). A reaction mixture consisting of rituximab (50–100 μ g) and iodine-125 (10–150 MBq) in binding buffer was prepared and dispensed into the coated microfuge tubes and these were left at room temperature for 20 min. The reaction was terminated by transferral of the solutions directly to either a fresh tube (for ITLC analysis using 10% TCA as the mobile phase to determine whether the reaction was complete) or to a PD-10 column that had previously been blocked with BSA and washed with either binding buffer or PBS. The radiolabelled protein was eluted with either binding buffer or PBS and 0.5 ml fractions were collected.

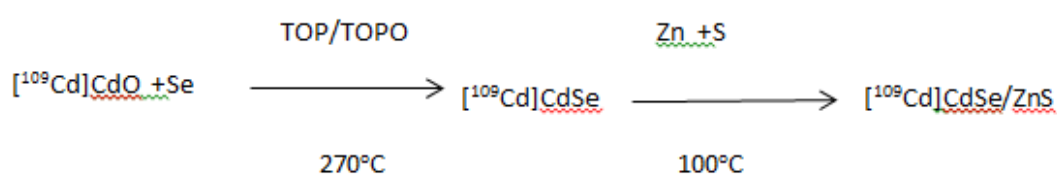
Bioconjugation to [125 I]Rituximab to carboxylated nanoparticles [21].

[109 Cd]CdSe/ZnS nanoparticles (200 μ L) were added to a solution of 1-ethyl-3-(3-dimethylaminopropyl)carbodiimide (EDC, 0.4 mg 2mM) and *N*-hydroxysulfosuccinimide (*N*-sulfo-NHS, 1.1mg, 5mM) in 0.1 M MES, 0.5M NaCl, pH 6.0 buffer and incubated at room temperature for 20 min. The reaction was then quenched by the addition of 2-mercaptoethanol (1.4 μ l, 20mM) and incubated at room temperature for 10 min. The activated [109 Cd]CdSe/ZnS were then adjusted to pH 7.0. The [125 I]Rituximab was then bio-conjugated to the [109 Cd]CdSe/ZnS. The protein, at a 2:1 to 5:1 molar ratio of biomolecule to dot, was dissolved in 1 ml PBS (1x, pH 7.5). The combined [109 Cd]CdSe/ZnS and [125 I]Rituximab solution was adjusted to pH 7.5 with NaOH and incubated at room temperature for 2 hours with continuous gentle mixing. Unconjugated [125 I]Rituximab was then removed by washing using a Nanosep 300k spin filter (Pall Corp. USA). In terms of final concentration, 1 mCi of Cd-109 is 3.5 nmol in 1 mL of solution. This would be equivalent would be 3.5 μ M. If the final particle concentration is 30 nM, this would give approximately 100

Cd-109 atoms in each nanoparticle. Gamma ray spectroscopy was then carried out on the [¹²⁵I]R1tuximab bioconjugated [¹⁰⁹Cd]CdSe/ZnS.

Results

This study aimed to develop a paradigm for tumour targeting and imaging using radiolabelled nanoparticles. The first step developed and optimized methods for the synthesis of [¹⁰⁹Cd]CdSe/ZnS water soluble quantum dots (Scheme 1).



Scheme 1. Synthesis of core/shell radio-nanoparticles.

Based upon the methods developed by Peng *et.al.*[14] and Nie. *et.al.*[15] the synthesis of CdSe/ZnS core/shell nanoparticles have been modified to allow the incorporation of the single photon emission computer tomographic (SPECT) isotope cadmium-109 to form [¹⁰⁹Cd]CdSe/ZnS core-shell quantum dots. The progress of the formation of the CdSe nanoparticles involving the introduction of [¹⁰⁹Cd]cadmium into the reaction melt was monitored by recording the UV spectra (Fig. 1a) and fluorescence spectra (Fig. 1b) of aliquots taken from the reaction vessel over the period of one minute.

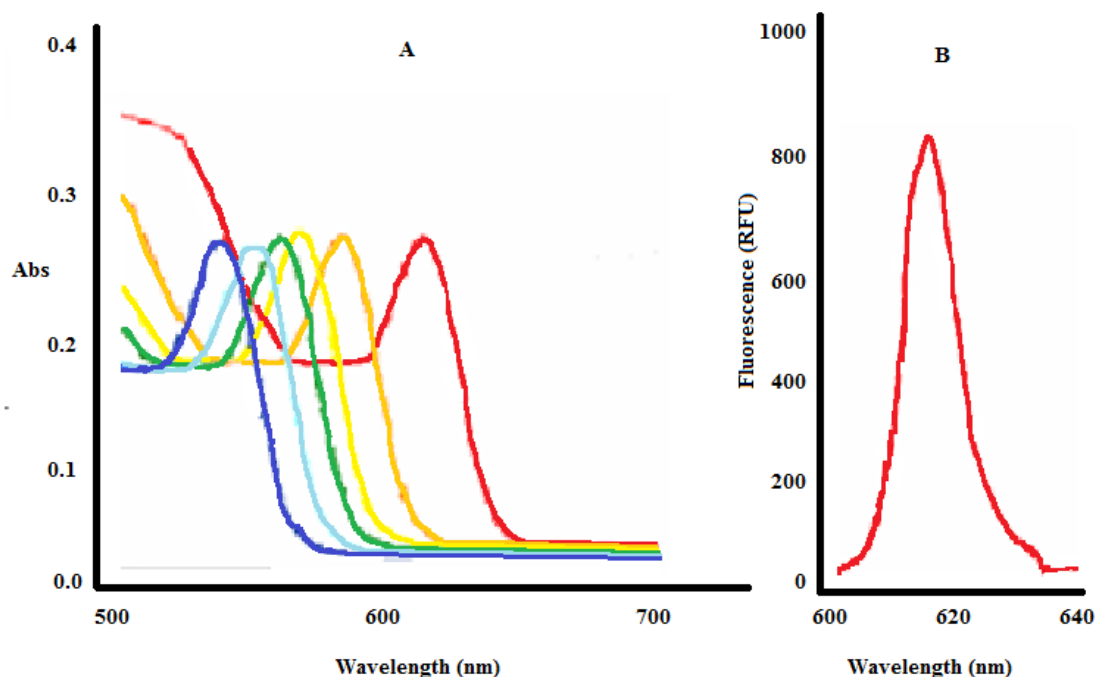


Figure 1a. UV spectra of $[^{109}\text{Cd}]\text{CdSe}$ nanoparticles. All of the reactions were performed under the same conditions, except the reaction time was increased by 10 seconds in each case. The Cd:Se molar ratio was 1:1. Figure 1b. Fluorescence of Carrier added CdSe nanoparticles.

These results obtained are consistent with the published literature[14,15] for stable CdSe nanoparticle production. This reaction was then repeated using tracer level cadmium only ($[^{109}\text{Cd}]\text{CdCl}_3$, 37MBq, 1mCi). The cadmium reaction concentrations equate to nmol levels of cadmium present in the reaction melt. All other parameters remained the same as in the carrier added reaction shown in Figure 1a and 1b. The reaction was monitored by recording the UV spectra (Fig. 2a) and fluorescence spectra (Fig. 2b) of aliquots taken from the reaction vessel over the period of one minute. However, no nanoparticle formation was observed over this time course. This is due to the greatly reduced concentration of cadmium-109 in the tracer only reaction reducing the reaction kinetics and slowing the formation of $[^{109}\text{Cd}]\text{CdSe}$. The reaction

melt was allowed to continue heating at 280°C for 1- 2 hours. Over this period of time the reaction melt slowly changed in colour from clear to red. Figure 2 shows UV and fluorescence analysis of the tracer level batch after 2 hours.

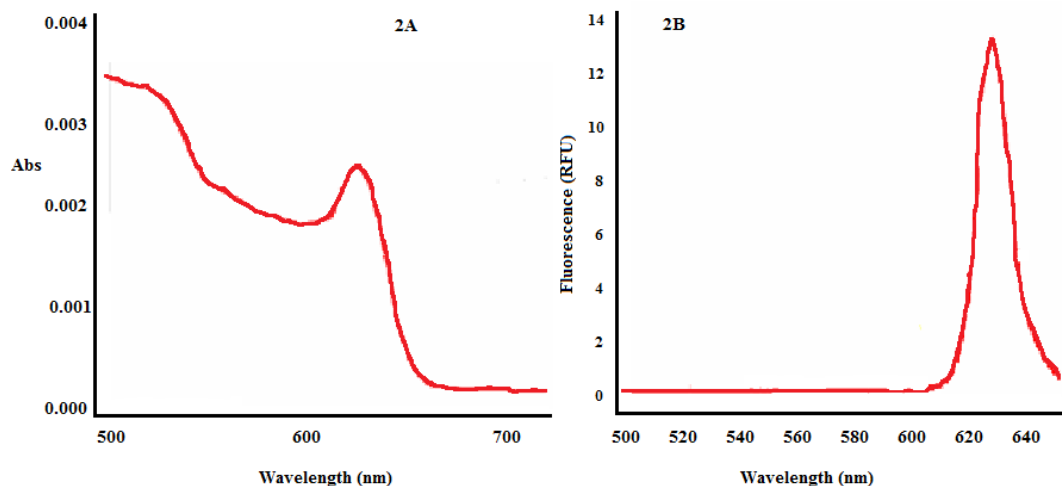


Figure 2. UV (2A) and fluorescence (2B) spectral analysis of the synthesis of tracer level $[^{109}\text{Cd}]\text{CdSe}$.

The first stage of synthesis using, either carrier added or tracer level, generated mono-dispersed $[^{109}\text{Cd}]\text{CdSe}$ nanoparticles ranging in size from 2-10nm, as demonstrated in the scanning electron micrograph (SEM) shown in Figure 3. These nanoparticles were synthesised using a high-temperature colloidal growth method followed by size selective precipitation with methanol[15,16].

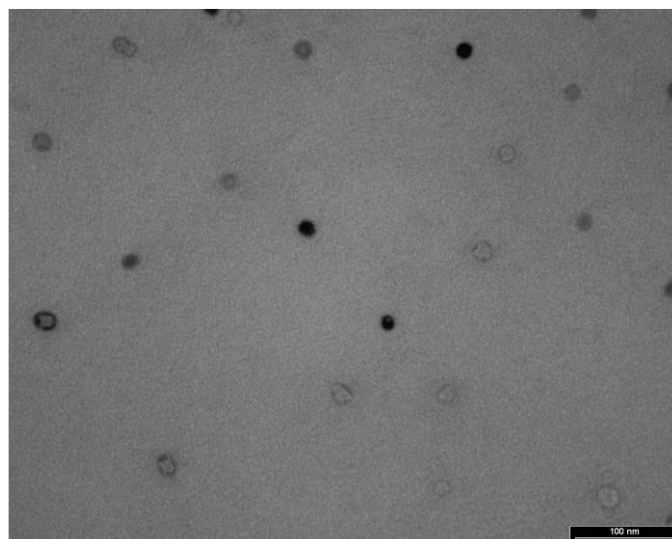


Figure 3. Scanning electron micrograph of the $[^{109}\text{Cd}]\text{CdSe}$ quantum dots produced by tracer level synthesis.

By using the extinction coefficients for CdSe published in the literature[21] ($\epsilon=3.7 \times 10^5 \text{ L/mol cm}$ for CdSe and $=3.5 \times 10^5 \text{ L/mol cm}$ for CdSe/ZnS at a path length 1 cm), for the first excitonic absorption peak (Fig. 1a and Fig. 2a) of the nanoparticles along with particle size analysis, which indicated a particle size of 5-10nm (Fig. 3), it has been possible to calculate the concentration of $[^{109}\text{Cd}]\text{CdSe}$ particles produced at both carrier added and tracer level. From the analysis, it was possible to deduce that the concentration of carrier added $[^{109}\text{Cd}]\text{CdSe}$ was approximately $3\text{-}4 \mu\text{molL}^{-1}$, whereas the concentration of tracer $[^{109}\text{Cd}]\text{CdSe}$ was estimated to be approximately $0.03\mu\text{molL}^{-1}$. Currently, the maximum permissible exposure dose for cadmium is $2.5 \mu\text{gkg}^{-1}$ of body weight[22].

These show that the concentration of nanoparticles at tracer level is approximately two orders of magnitude lower than the concentration of nanoparticles produced at carrier added level. However, the fluorescence spectra (Fig. 1b and Fig. 2b) of the

nanoparticles shows that even though smaller numbers of nanoparticles are produced over longer periods of time, they still retain their ability to fluoresce.

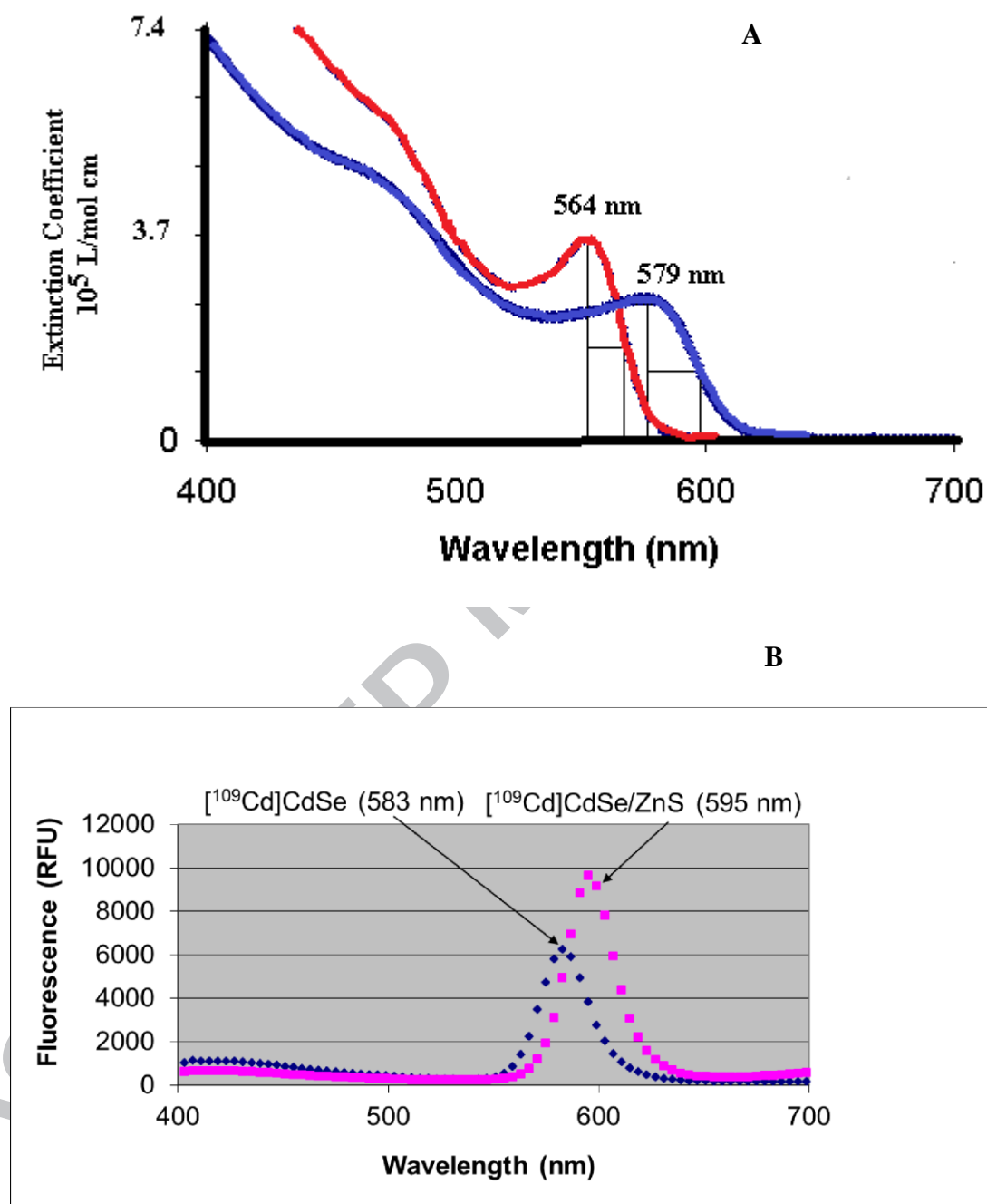


Figure 4. UV-vis (a) and fluorescence (b) analysis of $[^{109}\text{Cd}]\text{CdSe}$ and $[^{109}\text{Cd}]\text{CdSe/ZnS}$

Figure 4 also shows the comparison of absorption spectra (Fig. 4a) and fluorescence spectra (Fig. 4b) of $[^{109}\text{Cd}]\text{CdSe}$ core and $[^{109}\text{Cd}]\text{CdSe}/\text{ZnS}$ core-shell nanoparticle. It can be seen from the absorption spectra that when the nanoparticles are shelled with ZnS that there is an inherent redshift of 15nm[23]. We observed a shift in the absorption and fluorescence spectra (Fig. 4b) to the red (lower energies) after overcoating due to partial leakage of the exciton into the ZnS matrix[23].

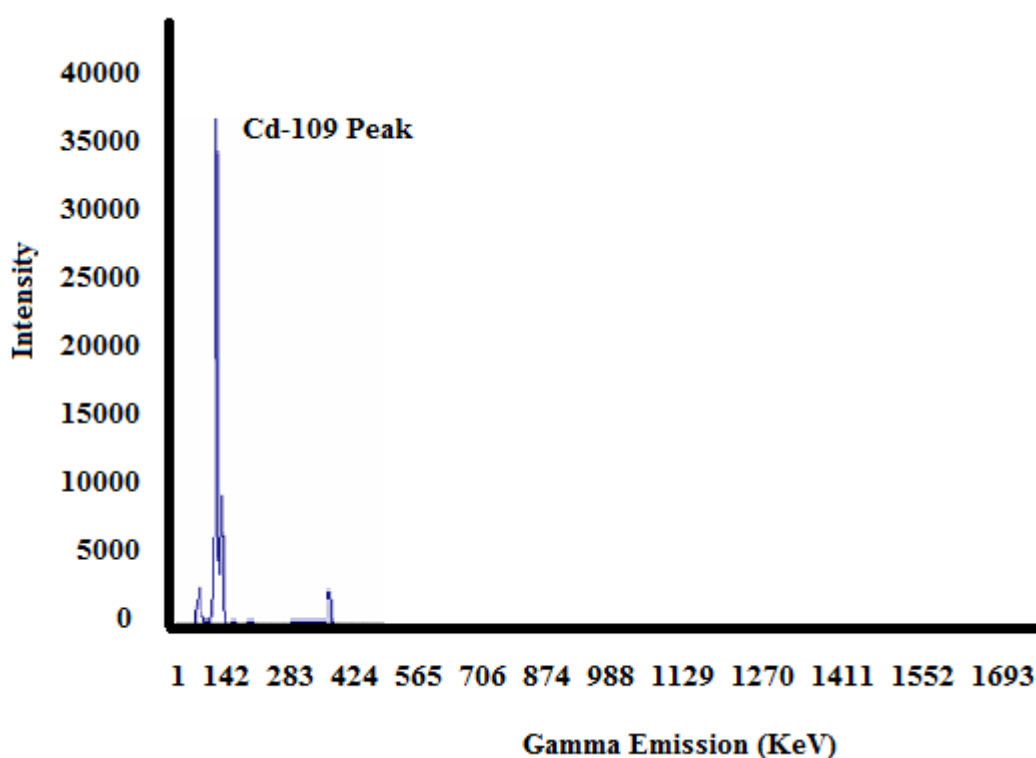


Figure 5. Gamm-ray spectroscopy of $[^{109}\text{Cd}]\text{CdSe}/\text{ZnS}$ nanoparticles

Gamma ray spectroscopy of the nanoparticles also indicates better than 90% uptake of the radioactive isotope in to the crystalline structure of the nanocrystal at tracer level synthesis (Figure 5).

Water dispersion of the $[^{109}\text{Cd}]\text{CdSe}/\text{ZnS}$ was carried out using mercaptoacetic acid, and tetramethylammonium hydroxide. Observation of the fluorescence after water dispersion clearly indicated a drop of 80-90% fluorescence emission from the dots

(Figure 6). This drop in fluorescence may be due to the decreased pH of the system quenching the nanoparticles [24]. However, gamma-ray spectroscopy indicated little loss of activity from the organic [^{109}Cd]CdSe/ZnS stage to the water dispersion stage.

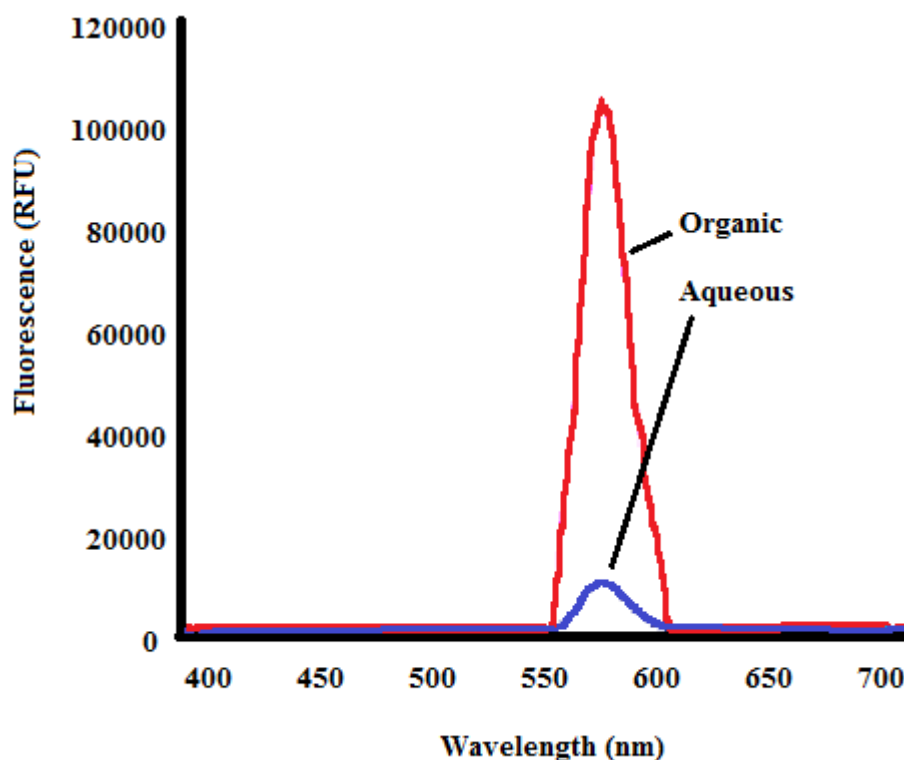


Figure 6. Loss in fluorescence during dispersion between organic and aqueous phase

Once the nanoparticles were rendered water dispersed it was necessary to bioconjugate the nanoparticles to a potential cancer marker which would demonstrate a possible future therapeutic application. The protein that was selected was the anti-CD-20 antibody rituximab[25]. This was done in order to demonstrate the potential biological uptake onto the surface of radio-nanoparticles. The reason for the selection of the Anti-CD-20 antibody rituximab, is that antibodies of this type have been successfully directed against cell surface targets and have already had a significant impact in oncology, cardiology, and immunology in the therapeutic realm[26]. The success of drugs such as rituximab attests to the ability of antibodies to localize and

engage or block critical biologic targets in patients. Also, rituximab has shown itself to be very amenable to radiolabelling for PET and SPECT scanning in the past.

In order to measure the percentage efficiency of protein binding to the $[^{109}\text{Cd}]\text{CdSe/ZnS}$, the rituximab was radiolabelled with the SPECT imaging agent I-125 which has distinct γ -rays at 35.5KeV[27]. The radioiodination process was carried out as described previously[27]. Gamma ray spectroscopy indicated $[^{125}\text{I}]\text{Rituximab}$ was bound to the $[^{109}\text{Cd}]\text{CdSe/ZnS}$ at the end of the bioconjugation process (Figure 7).

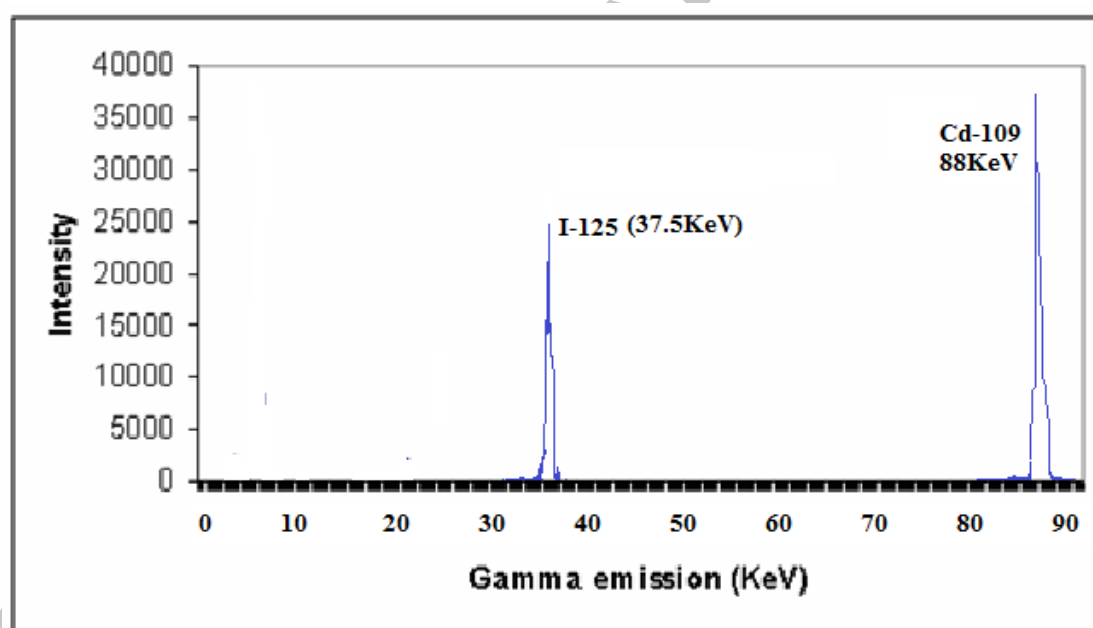


Figure 7 – Gamma ray spectrum of $[^{109}\text{Cd}]\text{CdSe/ZnS}-[^{125}\text{I}]\text{Rituximab}$

Overall γ -ray spectroscopy indicated that approximately 40% of the starting cadmium-109 was lost between the start of the synthesis of $[^{109}\text{Cd}]\text{CdSe}$ and the final bioconjugation wash (Figure 8).

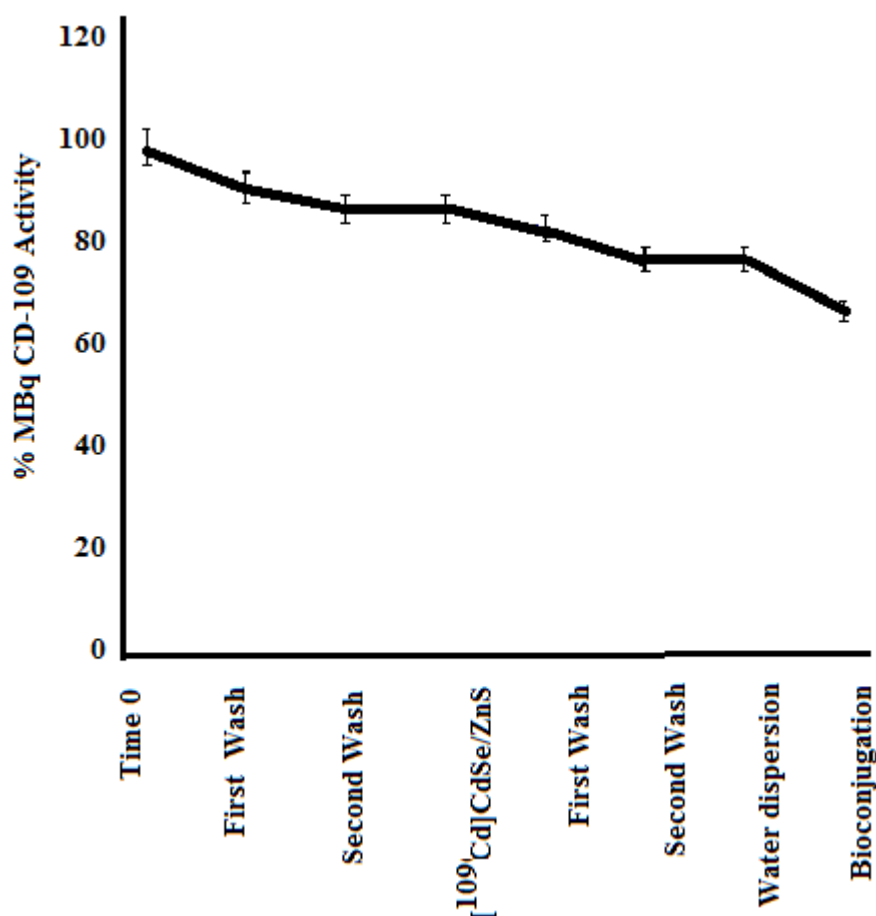


Figure 8. Loss profile of Cd-109 activity at each step in the synthesis.

Conclusion

This study demonstrates the synthesis of nanoparticles containing carrier free levels of a radioisotope used to form the nanoparticles, and subsequent bioconjugation of these nanoparticles to proteins of biological importance. In this case cadmium-109 was used. The nanoparticles produced were at tracer level, therefore, allowing the cadmium-109 SPECT imaging agent to be incorporated into a nanoparticle, which could allow for injection of the imaging agent into a subject at dramatically reduced levels of heavy metal toxicity. Currently, injection of a SPECT or positron emission tomographic (PET) radio imaging agent results in high signal to noise ratio, due to

high metabolism of the radiopharmaceutical. This metabolism may be reduced by locking the radioisotope in a stable crystalline structure, and coating the structure in a large number of molecules of the drug or targeting agent of interest. The incorporation of the tracer level radioisotope may also allow for a possible radiotherapeutic application, if enough radioactivity could be internally localised into the tumour.

References

1. Jin Xie, Seulki Lee, and Xiaoyuan Chen, Nanoparticle-based theranostic agents, *Adv Drug Deliv Rev.* **62**: (2010), 1064–1079.
2. Ulrik B. Nielsen and James D. Marks Internalizing antibodies and targeted cancer therapy: direct selection from phage display libraries., *Pharmaceutical Science & Technology Today*, 3, (2000), 282-291
3. Julian A. Kim, Targeted therapies for the treatment of cancer., *The American Journal of Surgery*, 186, (2003), 264-268.
4. Bruchez, M., Jr, Moronne, M., Gin, P., Weiss, S. & Alivisatos, A.P. Semiconductor nanocrystals as fluorescent biological labels. *Science* 281, (1998). 2013–2015
5. Akerman, M.E., Chan, W.C.W., Laakkonen, P., Bhatia, S.N. & Ruoslahti, E. Nanocrystal targeting *in vivo*. *Proc. Natl. Acad. Sci. USA* 99, (2002).12617–12621
6. Wu, X.Y. *et al.* Immunofluorescent labeling of cancer marker Her2 and other cellular targets with semiconductor QDs. *Nat. Biotechnol.* 21, (2003).41–46

7. Jaiswal, J.K., Mattoussi, H., Mauro, J.M. & Simon, S.M. Long-term multiple color imaging of live cells using quantum dot bioconjugates. *Nat. Biotechnol.* 21, (2003).47–51
8. Dahan, M. *et al.* Diffusion dynamics of glycine receptors revealed by single-quantum dot tracking. *Science* 302, (2003). 442–445
9. Rosenthal, S.J. *et al.* Targeting cell surface receptors with ligand-conjugated nanocrystals. *J. Am. Chem. Soc.* 124, (2002).4586–4594
10. Chan, W.C.W. & Nie, S.M. Quantum dot bioconjugates for ultrasensitive nonisotopic detection. *Science* 281, (1998).2016–2018
11. Chan, W.C.W. *et al.* Luminescent QDs for multiplexed biological detection and imaging. *Curr. Opin. Biotechnol.* 13, (2002).40–46
12. Alivisatos, A.P. Semiconductor clusters, nanocrystals, and quantum dots. *Science* 271, (1996). 933–937
13. Reiss, P., Carrière, M., Lincheneau, C., Vaure, L., Tamang, S., Synthesis of Semiconductor Nanocrystals, Focusing on Nontoxic and Earth-Abundant Materials, *Chem. Rev.* 116, (2016). 10731-10819
14. Peng, Z.A. & Peng, X. Formation of high-quality CdTe, CdSe, and CdS nanocrystals using CdO as precursor. *J. Am. Chem. Soc.* 123, (2001).183–184
15. Nie, S. *et al.* Quantum-dot-tagged microbeads for multiplexed optical coding of biomolecules. *Nat. Biotechnol.* 19, (2001).631–635
16. Gao, X. *et al.* In vivo cancer targeting and imaging with semiconductor quantum dots. *Nat. Biotechnol.* 22. (2004). 969 – 976
17. Lidke, D.S. *et al.* Quantum dot ligands provide new insights into erbB/HER receptor-mediated signal transduction. *Nat. Biotechnol.* 22, (2004). 198–203

18. Chang JC, Kovtun O, Blakely RD, Rosenthal SJ., Labeling of neuronal receptors and transporters with quantum dots., *Rev Nanomed Nanobiotechnol.* **6** (2012), 605-19.
19. Jonathan C. Claussen, Anthony Malanoski, Joyce C. Breger, Eunkeu Oh, Scott A. Walper, Kimihiro Susumu, Ramasis Goswami, Jeffrey R. Deschamps, and Igor L. Medintz., Probing the Enzymatic Activity of Alkaline Phosphatase within Quantum Dot Bioconjugates., *The Journal of Physical Chemistry C*, **119** (2015). 2208-2221.
20. Yezhelyev MV, Qi L, O'Regan RM, Nie S, Gao X. Proton-sponge coated quantum dots for siRNA delivery and intracellular imaging. *J Am Chem Soc.*, **130**, (2008)., 9006–9012.
21. Sun. J., and Goldys, E.M., Linear Absorption and Molar Extinction Coefficients in Direct Semiconductor Quantum Dots., *J. Phys. Chem. C*, **112**, (2008) 9261–9266
22. IARC monographs on the evaluation of carcinogenic risk of chemicals to humans, (1993). vol. 58. Lyon, France, pp 444
23. Cingarapu, S., Yang, Z., Sorensen, C.M., and Klabunde K.J., Synthesis of CdSe/ZnS and CdTe/ZnS Quantum Dots: Refined Digestive Ripening. *Journal of Nanomaterials.*, (2012), pp.1-12
24. Ji, X., Palui, G., Avellini, T., Bin Na, H., Yi, C., Knappenberger, K.L., and Mattoussi, H., On the pH-Dependent Quenching of Quantum Dot Photoluminescence by Redox Active Dopamine, *Journal of the American Chemical Society* **134**, (2012)., 6006-6017
25. Weiss, A., Preston, T.C., Popov, J., Li, Q., Wu, S., Chou, K.C., Burt, H.M., Bally, M.B., and Signorell, R., Selective Recognition of Rituximab-

Functionalized Gold Nanoparticles by Lymphoma Cells Studied with 3D Imaging., *The Journal of Physical Chemistry C*, **113**, (2009), 20252-20258

26. Wu, A.M., Antibodies and Antimatter: The Resurgence of Immuno-PET, *J Nucl Med.* (2009);**50**:2-5
27. Hall, B, Heynen M, Jones LW, Forrest JA. Analysis of Using I(125) Radiolabeling for Quantifying Protein on Contact Lenses., *Curr Eye Res.* **41** (2016)., 456-65

Conflict of interest statement: The author declares no competing financial interest

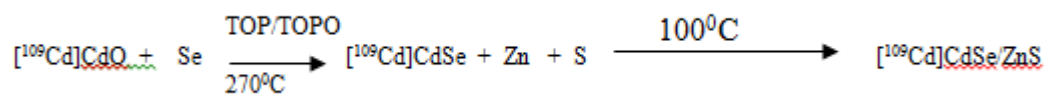
Funding Sources: This work was funded by Cancer Research UK and the University of Manchester.

A

Highlights

- This work describes the synthesis and analysis of radioactive multifunctional nanoparticle probes based on CdSe/ZnS semiconductor quantum dots (QDs) for potential *in vitro* and *in vivo* anti-cancer theranostics.
- The synthetic design involved the radiosynthesis of luminescent CdSe/ZnS QDs using the SPECT imaging agent Cd-109 as the cadmium elemental source.
- These radioactive nanoparticle materials were then rendered water soluble and bioconjugated to the tumor-targeting ligand Retuximab.

Graphical Abstract



This work describes the synthesis and analysis of radioactive multifunctional nanoparticle probes based on [¹⁰⁹Cd]CdSe/ZnS semiconductor quantum dots (QDs) for potential *in vitro* and *in vivo* anti-cancer theranostics.